

Pulsed field-ionization photoelectron-photoion coincidence study of the process $N_2 + h\nu \rightarrow N^+ + N + e^-$: Bond dissociation energies of N_2 and N_2^+

Xiaonan Tang, Yu Hou, and C. Y. Ng^{a)}

Department of Chemistry, University of California, Davis, California 95616

Branko Ruscic^{b)}

Chemistry Division, Argonne National Laboratory, Argonne, Illinois 60639-4831

(Received 13 May 2005; accepted 15 June 2005; published online 25 August 2005)

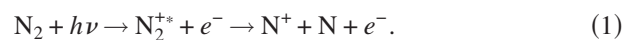
We have examined the dissociative photoionization reaction $N_2 + h\nu \rightarrow N^+ + N + e^-$ near its threshold using the pulsed field-ionization photoelectron-photoion coincidence (PFI-PEPICO) time-of-flight (TOF) method. By examining the kinetic-energy release based on the simulation of the N^+ PFI-PEPICO TOF peak profile as a function of vacuum ultraviolet photon energy and by analyzing the breakdown curves of N^+ and N_2^+ , we have determined the 0-K threshold or appearance energy (AE) of this reaction to be 24.2884 ± 0.0010 eV. Using this 0-K AE, together with known ionization energies of N and N_2 , results in more precise values for the 0-K bond dissociation energies of N–N (9.7543 ± 0.0010 eV) and N– N^+ (8.7076 ± 0.0010 eV) and the 0-K heats of formation for N (112.469 ± 0.012 kcal/mol) and N^+ (447.634 ± 0.012 kcal/mol). © 2005 American Institute of Physics. [DOI: 10.1063/1.1995699]

I. INTRODUCTION

One of the most valuable thermochemical data that can be obtained in single-photon vacuum ultraviolet (vuv) photoionization-photoelectron measurements is the 0-K threshold or appearance energy (AE) of a dissociative photoionization process.¹ The recent introduction of the high-resolution pulsed field-ionization photoelectron (PFI-PE)-photoion coincidence (PFI-PEPICO) time-of-flight (TOF) method² has allowed the determination of 0-K AE values for many dissociative photoionization processes of simple molecules with unprecedented precision (≈ 0.1 kJ/mol), which is limited mostly by the precision achieved in PFI-PE measurements.^{3–14}

As pointed out in previous PFI-PEPICO TOF studies, the analysis of the breakdown curves measured in PEPICO TOF experiments represents one of the most reliable methods for 0-K AE determinations.^{1–4} Because the 0-K AE is distinctly marked by the disappearance energy of the parent ion observed in the breakdown diagram regardless the temperature of the gas sample, the 0-K AE value can be determined without any simulations.^{1–4} Furthermore, the PFI-PEPICO TOF peak for the daughter ion contains information about the kinetic-energy release.¹² By measuring the kinetic-energy release based on the simulation of the daughter PFI-PEPICO TOF peak as a function of vuv photoionization energy or internal excitation of the parent ion, we have previously identified the dissociative photoionization for the formation of $O^+ + CO$ and $CO^+ + O$ from CO_2 .¹²

Here, we report the result of a PFI-PEPICO TOF study of the dissociative photoionization process,



When the excited diatomic cation such as N_2^{+*} with a fixed internal energy dissociates near the dissociation threshold such that the atomic fragments $N^+ + N$ are produced in their ground states, there can only be one single kinetic-energy release because the atomic fragments cannot possess rovibrational energies. As a result, the analysis of the measured PFI-PEPICO TOF peak of the daughter N^+ ion by varying the vuv photoionization energy ($h\nu$) becomes a very sensitive mean for the determination of the 0-K AE of process (1). The combined kinetic-energy release and breakdown curve measurements have yielded a highly precise 0-K AE(N^+) from N_2 . Because the ionization energies (IEs) for N and N_2 have been very precisely measured,^{15–17} the 0-K bond dissociation energies (D_0 's) for N–N and N^+ –N can be obtained by the relations,

$$D_0(N^+ - N) = AE(N^+) - IE(N_2), \quad (2)$$

$$D_0(N - N) = AE(N_2^+) - IE(N). \quad (3)$$

The primary motivation for the present investigation is to try to establish an improved value for $D_0(N - N)$, and hence $\Delta H_f^\circ(N)$. The current experimental value^{18–21} for $\Delta H_f^\circ(N)$ is derived from $D_0(N - N) = 78\,715 \pm 50$ cm^{–1} (225.057 ± 0.143 kcal/mol) (Refs. 22–25) obtained by Buttenbender and Herzberg. The need to improve this quantity has surfaced recently while building and analyzing the Core (Argonne) Thermochemical Network [C(A)TN], which is currently being developed as a separate effort and is the basis for Active Thermochemical Tables (ATcT).^{26,27} ATcT, are a new approach that allows the derivation of accurate, reliable, and internally consistent thermochemical values. In contrast with traditional (sequential) thermochemistry, ATcT extract

^{a)}Electronic mail: cyng@chem.ucdavis.edu

^{b)}Electronic mail: ruscic@anl.gov

the thermochemical values of interest by statistically analyzing, iteratively optimizing, and solving a thermochemical network (TN) that is constructed from all the relevant thermochemical determinations and explicitly exposes and utilizes the interdependencies between various thermochemical quantities. Besides producing thermochemical values that are based on full and optimal utilization of the aggregate knowledge stored in the TN, ATcT offer a number of additional features that are neither present nor possible in the traditional approach, such as easy propagation of new knowledge with a concomitant automatic update of all affected thermochemical values, availability of the full covariance matrix detailing the interdependencies of values, a hypothesis testing and evaluation capability, etc. In particular, an inspection of the computed statistical measures (such as the covariance matrix and the sensitivity matrix) that are obtained by analyzing and manipulating the current C(A)TN, combined with insights into the TN topology, can lead to the isolation of “weak” links in the network, thereby generating pointers to the highly desired experimental or computational determinations that will efficiently improve the knowledge content of the TN.^{26,27} One such current “weak link” is the value of $D_0(\text{N}-\text{N})$, which is the primary contributor to the resulting value of the enthalpy of formation of atomic nitrogen, $\Delta H_f^\circ(\text{N})$ and presently limits its accuracy. The latter enthalpy of formation is one of the global “key” thermochemical values, and is the pivoting quantity for the establishment of accurate enthalpies of formation of NO and NO₂ through $D_0(\text{NO})$ and $D_0(\text{O}-\text{NO})$. Propagating further through the inherent thermochemical interdependencies, $\Delta H_f^\circ(\text{NO})$ and $\Delta H_f^\circ(\text{NO}_2)$ are in turn pivoting quantities responsible for the enthalpies of formation of the other nitrogen oxides, NO_x, further affecting the thermochemistry of the chemical species with the formula H_xN_yO_z, and so on. The value (and the uncertainty) for $\Delta H_f^\circ(\text{N})$, is also of pivotal importance as a fixed reference value for all electronic structure computations of that derive the enthalpy of formation through computed atomization energies (such as the high-accuracy composite methods from the Gn family developed by Curtiss *et al.*²⁸ or the Wn family recently developed by Martin and de Oliveira²⁹). Clearly, in all these cases the value and uncertainty of $\Delta H_f^\circ(\text{N})$ affects the value and uncertainty of the enthalpies of formation of the target nitrogen-containing chemical species, and, in fact, this contribution scales linearly with the number of nitrogen atoms in the target species.

II. EXPERIMENTAL CONSIDERATIONS

The PFI-PEPICO TOF experiments were carried out using the high-resolution vuv photoelectron-photoion facility of the chemical dynamics beamline at the advanced light source³⁰ (ALS) which was operated in the multibunch mode (synchrotron ring period=656 ns, dark gap=84 ns). The facility consists of a 10-cm period undulator, a gas harmonic filter, a windowless 6.65-m off-plane Eagle mounted monochromator, and a multipurpose photoelectron photoion apparatus.^{1,31,32} In the present experiment, helium was used in the harmonic gas filter to suppress higher undulator harmonics with photon energies greater than 24.59 eV. A

2400-lines/mm grating (dispersion=0.64 Å/mm) was used to disperse the first-order harmonic of the undulator vuv beam with entrance/exit slits set in the range of 20–100 μm. The resulting monochromatic vuv beam was then focused into the photoionization/photoexcitation (PI/PEX) region of the photoelectron-photoion apparatus.

The photon energy calibration was achieved using the Ne⁺(²P_{3/2}, ²P_{1/2}) and He⁺(²S) PFI-PE bands. The calibration scheme assumes that the Stark shifts of the ionization energies (IEs) of N₂ and rare gases are identical. On the basis of previous experiments, the accuracy of the energy calibration is shown to be within ±0.5 meV.³³

The schematic diagram of photoelectron-photoion coincidence spectrometer, typical voltages applied to individual lenses, and the procedures for PFI-PEPICO measurements have been described in detail previously.² The PFI-PEPICO TOF spectra were measured in the photon energy region 23.58–24.35 eV. A dc field of 0.2 V/cm was used at the PI/PEX region to disperse the prompt electrons. The PFI at the PI/PEX region was achieved by applying an electric pulse (height=9 V/cm, width=200 ns) at the dark gap of the synchrotron period. The PFI electric pulse also served to extract PFI photoions toward the ion detector.² The average accumulation time for one PFI-PEPICO spectrum is about 50–60 min. The PFI-PEPICO resolution achieved is 1.0 meV [full width at half maximum (FWHM)]. The N₂ sample was introduced into the PI/PEX region as a continuous, neat N₂ supersonic beam at a total stagnation pressure of 760 Torr. The molecular beam was skimmed by a circular skimmer (diameter=1 mm) before entering the photoionization chamber. The alignment of the nozzle and the skimmer was adjusted to give the lowest translational temperature (≈5 K) for N₂ as measured by the width of the N₂⁺ PFI-PEPICO TOF peak. During the experiment, the beam source chamber and the photoionization chamber were maintained at 5 × 10⁻⁴ and 5 × 10⁻⁷ Torr, respectively.

III. RESULTS AND DISCUSSION

Two methods are adopted to determine the 0-K AE of N⁺ from N₂ [process (1)]: One is based on the measured breakdown curves for N⁺ and N₂⁺, and the other relies on the kinetic energy release analysis of the observed PFI-PEPICO TOF peak profiles for N⁺ and N₂⁺.

A. Breakdown curves for N⁺ and N₂⁺

An illustrative set of selected PFI-PEPICO TOF spectra obtained at $h\nu=23.5810$, 24.2672, 24.2871, 24.2881, 24.2888, and 24.2891 eV, are shown in Figs. 1(a)–1(f). At 23.5810 eV, which is well below the dissociative photoionization threshold of process (1), only the parent TOF peak is observed at 20.85 μs. The spectrum at 24.2672 eV [Fig. 1(b)] reveals the fragment N⁺ TOF peak at 14.65 μs in addition to the parent ion TOF peak. The broadness of this N⁺ TOF peak indicates that the fragment N⁺ ions result mostly from dissociative photoionization of ambient thermal N₂ neutrals in the photoionization chamber. The exceptionally high intensity observed for this N⁺ TOF peak is consistent with the lifetime switching effect⁵ at energies very slightly

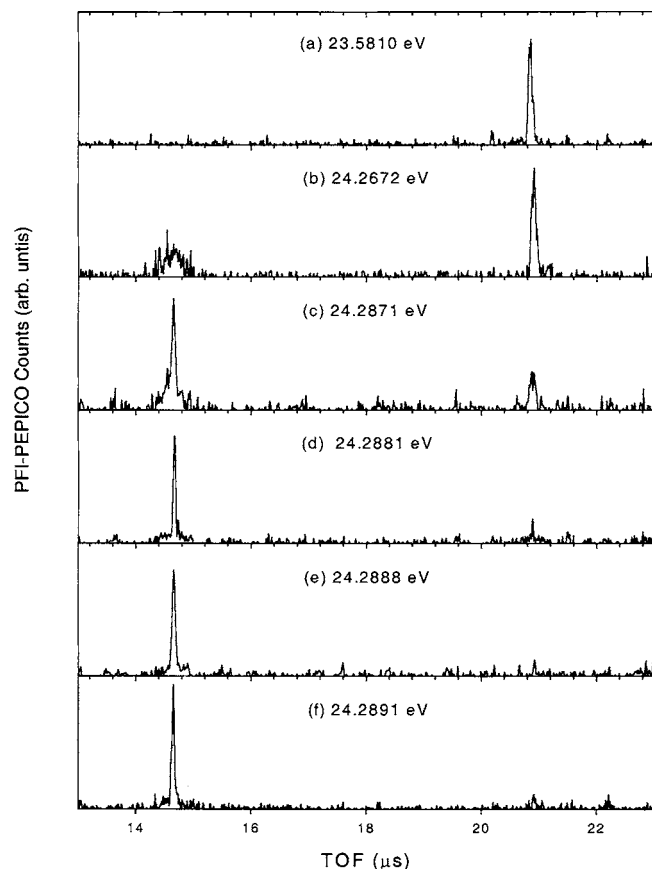


FIG. 1. Selected PFI-PEPICO TOF spectra for N_2^+ and N^+ observed at VUV photoionization energies of (a) 23.5810, (b) 24.2672, (c) 24.2871, (d) 24.2881, (e) 24.2888, and (f) 24.2891 eV.

below to the dissociative photoionization threshold. This effect has been observed and discussed in many previous studies.^{3–7,11} Briefly, the lifetime switching effect occurs because excited N_2 in a high- n ($n > 100$) Rydberg state [$N_2^*(n)$] formed by vuv excitation at energies slightly below the threshold for process (1) dissociates promptly into $N^*(n') + N$ prior to PFI by the application of the PFI electric-field pulse. Here $N^*(n')$ represents excited N in a high- n' Rydberg state. Since $N^*(n')$ is below the IE(N) and cannot autoionize, the lifetime of $N^*(n')$ is longer than that of $N_2^*(n)$, which is well above the IE(N_2). The fact that the PFI-PE signal observed at energies slightly below the 0-K AE(N^+) for process (1) arises from PFI of $N^*(n')$ accounts for the enhancement observed of the PFI-PEPICO TOF peak for the fragment N^+ ion in Fig. 1(b). As the vuv energy is increased to 24.2871 eV, the PFI-PEPICO TOF peak for fragment N^+ can be seen to consist of contributions from a broad thermal N_2 component and a narrow supersonically cooled N_2 component and becomes dominant compared to that for N_2^+ [see Fig. 1(c)]. The PFI-PEPICO TOF spectra observed at vuv energies ≥ 24.2881 eV reveal only a negligibly small TOF peak for N_2^+ as shown in Figs. 1(d)–1(f). A quantitative analysis of the TOF profile at 23.5810 eV shows that the thermal N_2^+ signal is about 10%–15% of the N_2^+ signal. The thermal N^+ signals are found to increase to 42% and 50% of the total N^+ and N_2^+ signal at 24.2672 and 24.2871 eV, re-

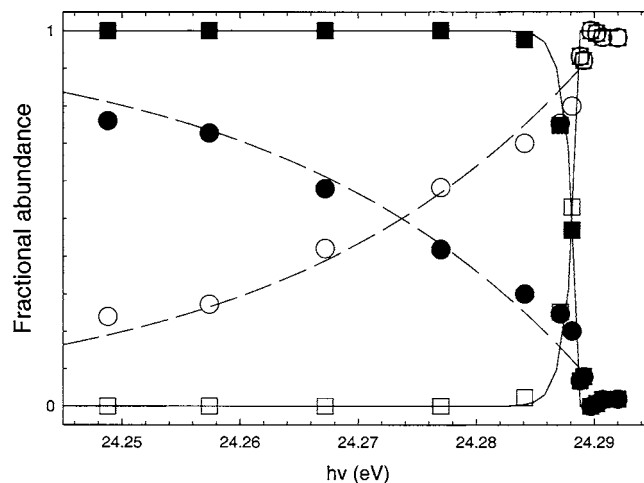


FIG. 2. Breakdown curves of N^+ and N_2^+ in the VUV photon energy ($h\nu$) range of 24.2488–24.2920 eV. The fractional abundances for N^+ and N_2^+ are constructed using the integrated ion signals under the PFI-PEPICO TOF peaks for N^+ and N_2^+ as the intensities for N^+ and N_2^+ , respectively. The open and closed circular symbols show the respective fractional abundances of N^+ and N_2^+ derived by taking into account the cold and thermal components of N^+ . The dashed lines are simulated curves assuming an effective temperature of 300 K for N_2^+ . The open and closed rectangular symbols show the respective fractional abundances of N^+ and N_2^+ derived by taking into account only the cold components of N^+ . The solid lines are simulated assuming a temperature at 10 K for N_2^+ .

spectively. The thermal N^+ signal drops to 23% and 15% of the total N^+ and N_2^+ signal at 24.2888 and 24.2891 eV, respectively.

The respective integrated ion signals under the PFI-PEPICO TOF peaks for N^+ and N_2^+ were taken as the intensities of N^+ [$I(N^+)$] and N_2^+ [$I(N_2^+)$]. The fractional abundances of N^+ and N_2^+ are determined as $I(N^+)/[I(N^+) + I(N_2^+)]$ and $I(N_2^+)/[I(N^+) + I(N_2^+)]$, respectively. The breakdown curves for N^+ and N_2^+ , i.e., the fractional abundances for N^+ (open circles) and N_2^+ (solid circles) plotted as a function of $h\nu$ in the range of 24.25–24.29 eV, are depicted in Fig. 2. As expected, the fractional abundance for the parent N_2^+ ion decreases as the $h\nu$ is increased with the concomitant increase in the fractional abundance of the daughter N^+ ion. We note that the breakdown curves for N^+ and N_2^+ constructed based on the intensities determined by the total TOF peak area have included contributions from both the cold and thermal components of N_2 . The dashed lines are simulated breakdown curves obtained using a procedure described previously³⁴ and assuming an effective rotational temperature of 300 K for N_2 . Since the PFI-PEPICO TOF spectra resolve the dissociation due to cold N_2 from those of thermal N_2 , we have also constructed the breakdown diagram based only on the intensities of the cold N^+ and N_2^+ components. The open and closed rectangular symbols in Fig. 2 show the respective fractional abundances of N^+ and N_2^+ determined by using only the cold components of N^+ and N_2^+ . As expected, the breakdown curves constructed based on the dissociation of cold N_2^+ formed by photoionization of supersonically cooled N_2 are much sharper. The solid curves of Fig. 2 represent the simulated curves obtained by assuming a rotational temperature of 10 K for the cold component of N_2 .

As pointed out in previous PFI-PEPICO studies,^{1–14} the

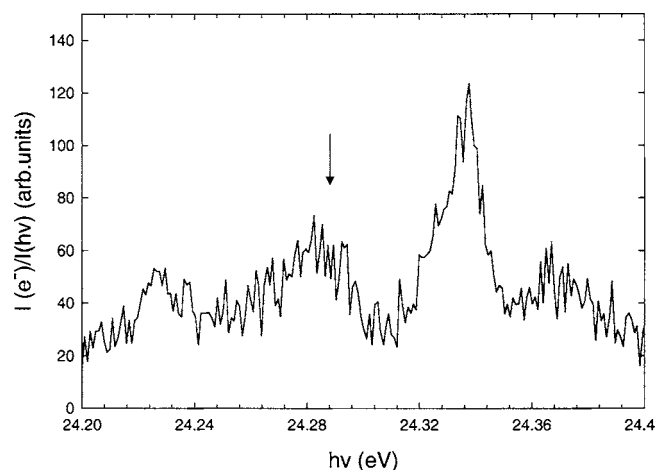


FIG. 3. PFI-PE spectrum of N_2 in the VUV region of 24.20–24.40 eV. The position of the downward arrow represents the 0-K AE(N^+) from N_2 determined in the present PFI-PEPICO TOF study.

0-K AE can be unambiguously determined by the disappearance energy of the parent ion. The dispersion of hot electrons into the dark gap of the synchrotron ring period can give rise to coincidence background for N_2^+ . In such cases, we have shown that the disappearance energy is manifested as a sharp break in the breakdown curve for the parent ion, where the breakdown curve of the parent ion reaches its lowest value and levels off. The break in the breakdown curve for the parent N_2^+ ion is clearly observed at 24.2888 eV, where the intensity of the TOF peak for parent N_2^+ is found to be within the noise level. We note that the dark gap (84 ns) of the synchrotron ring period used in the present experiment is narrower than that (104 ns) used previously. Consequently, the small residual N_2^+ signal (fractional abundance ≤ 0.03) observed at energies ≥ 24.2888 eV is likely due to be the dispersion of prompt electrons into the dark gap of the synchrotron ring period. Taking into account the error of ± 0.5 meV for vuv energy calibration, we conclude from this set of measurements that the 0-K AE(N^+) for process (1) is 24.2888 ± 0.0010 eV, where the uncertainty reflects an estimated 95% confidence interval.

In PFI-PEPICO measurements of polyatomic systems, where the density of states is high, the lifetime switching effect is manifested as a step in the PFI-PE spectrum at the 0-K AE of the dissociative photoionization process.^{1,3–7} In the study of CO_2 , a peak in the PFI-PE spectrum is found to coincide with each of the 0-K AE for the formation of $O^+(^4S) + CO(X^1\Sigma^+)$ and $CO^+(X^2\Sigma^+) + O(^3P)$ from CO_2 .¹² Similarly, peaks are observed in the PFI-PE spectrum at energies coincide with the 0-K AEs for the dissociative photoionization processes $CS_2 + h\nu \rightarrow S^+(^4S) + CS(X^1\Sigma^+; v=0 \text{ and } 1) + e^-$.³⁵ We have measured the PFI-PE spectrum for N_2 in the region of 23.40–24.40 eV using a PFI-PE resolution of 5 cm^{-1} (FWHM).³⁶ The PFI-PE spectrum of N_2 thus observed reveals many vibrational bands of the N_2^+ (X , C , and $2^2\Pi_g$) states. These PFI-PE vibrational bands are found to superimpose on a continuous component of PFI-PE signals with significant intensities, indicating that the PFI-PE spectrum is mediated by dissociative states of N_2 . Figure 3 depicts the PFI-PE spectrum of N_2 recorded in the region of

24.20–24.40 eV. The prominent PFI-PE peak at 24.338 eV can be ascribed to the vibrational band of the $N_2^+(C)$ state. Other minor peaks could have contributions from vibrational bands of the $N_2^+(2^2\Pi_g)$. The fact that the 0-K AE for process (1) (marked by the downward arrow in Fig. 3) coincides with the PFI-PE peak at 24.2885 eV suggests that the latter PFI-PE peak arises mostly from the lifetime switching effect.

B. Kinetic-energy release analysis

When a dc field E (V/cm) is maintained at the photoionization region, the width (ΔT) of the N^+ PFI-PEPICO TOF peak can be calculated as³⁷

$$\Delta T = \frac{\sqrt{8m(E_{KE} + E_T)}}{qE}, \quad (4)$$

where, m and q represent the mass and the electric charge of N^+ , respectively; E_{KE} is the kinetic energy gained by N^+ due to the energy release of reaction (1); and E_T represents the thermal translational energy of N^+ , which is determined by the translational temperature of N_2 along the TOF axis. Equation (4) can also be expressed as

$$E_{KE} = \left(\frac{q^2 E^2}{8m} \right) (\Delta T)^2 - E_T. \quad (5)$$

In the present experiment, instead of using a dc electric field, a pulsed electric field was employed to the repeller to extract the N^+ and N_2^+ ions.² The kinetic energy for N^+ can be obtained by simulation of the observed TOF peak using the SIMION program.^{38,39} The simulation indicates that Eq. (4) can be used to calculate the kinetic energy for N^+ with only minor discrepancies if E is replaced by the effective dc field (E_{eff}) of 2.74 V/cm, which is calculated as (amplitude of the PFI pulse = 9.0 V/cm) \times (PFI pulse width = 200 ns) / (synchrotron ring period = 656 ns).

The parent N_2^+ ion in PEPICO measurements are all produced in the PFI of $N_2^*(n)$ formed by vuv excitation of N_2 . Thus, the cold component of the N_2^+ PFI-PEPICO TOF peak is expected to be decided solely by the N_2 supersonic beam temperature, which does not change with respect to $h\nu$. This expectation is supported by the observation that the FWHM for the PFI-PEPICO TOF peak of N_2^+ in the $h\nu$ range from 24.257 to 24.287 eV is constant (see Fig. 4). As indicated above, the TOF peaks for N_2^+ are dominated by contributions from N_2 in the supersonic beam. The simulation^{2,12} of the TOF peak profiles for parent N_2^+ ions observed in the vuv energy range of 24.257–24.287 eV yields a translational temperature of ≈ 5 K for the supersonically cooled N_2 beam.

The FWHMs observed for the TOF peaks of N^+ in the vuv energy range of 24.2574–24.2977 eV are also depicted in Fig. 4. The high FWHM values for the N^+ TOF peaks observed at 24.257–24.287 eV are consistent with the fact that the N^+ ions produced at these energies are contributed predominantly by the dissociative photoionization of thermal N_2 existing in the photoionization chamber. As the $h\nu$ is increased, the dissociation from the supersonically cooled N_2 component increases, resulting in narrower FWHMs for TOF peaks of N^+ . The TOF peak width should reach its minimum value at the 0-K AE of process (1). The further increase in

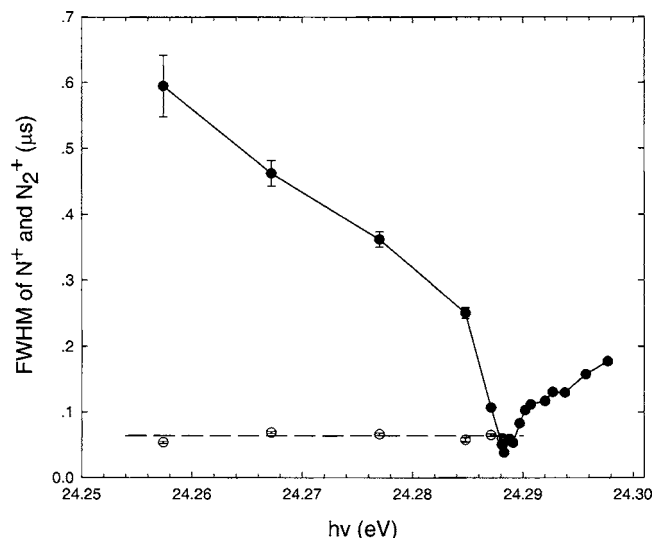


FIG. 4. Comparison of the full width at half maximum (FWHMs) of the N^+ (filled circles) and N_2^+ (open circles) PFI-PEPICO TOF peaks in the range of 24.257–24.300 eV. The FWHMs of the N_2^+ TOF peaks correspond to a translational temperature of 5 K for N_2^+ .

vuv energy from the 0-K AE gives rise to a finite kinetic-energy release, and thus is expected to broaden the TOF peak of N^+ . As shown in Fig. 4, the FWHM is found to increase as vuv is increased from 24.2883 to 24.2977 eV. On the basis of the argument presented above, we can conclude that the 0-K AE for process (1) is 24.2883 ± 0.0010 eV, where the TOF peak of N^+ has the narrowest width. The assigned error of ± 0.0010 eV has taken into account the error of vuv energy calibration and reflects an estimated 95% confidence interval.

Assuming that the dissociative photoionization of N_2 involves two consequential steps 1(a) (photoionization step to produce an excited N_2^{+*} ion and a zero kinetic-energy electron) and 1(b) (N_2^{+*} dissociation to produce N^++N), the appearance energy and the observed total kinetic-energy release (KER= $2E_{KE}$) for process (1) at energy $h\nu$ are related as

$$AE(N^+) = h\nu - 2E_{KE}. \quad (6)$$

The magnified views of the PFI-PEPICO TOF peaks observed for N^+ at $h\nu=24.2883$, 24.2888, 24.2907, 24.2938, and 24.3365 eV are shown in Figs. 5(a)–5(e), respectively. We have simulated^{2,12} these TOF peaks for N^+ (produced from N_2^+ at a translational temperature of 5 K) to determine the kinetic-energy release (E_{KE}). The best-fitted curves (solid line) are also shown in Figs. 5(a)–5(e). The KER values determined at $h\nu=24.2883$, 24.2888, 24.2907, 24.2938, and 24.3365 eV are given in Table I. The 0-K AE values calculated using Eq. (6) at individual $h\nu$ values are also listed in Table I. The mean 0-K AE is 24.2880 eV with a standard deviation of the sample of 0.0008, the standard deviation of the mean of 0.0003, and the 95% confidence limit interval of 0.0009 eV.

C. Thermochemistry

On the basis of the breakdown curves for N^+ and N_2^+ or the disappearance energy of N_2^+ observed in the PFI-PEPICO

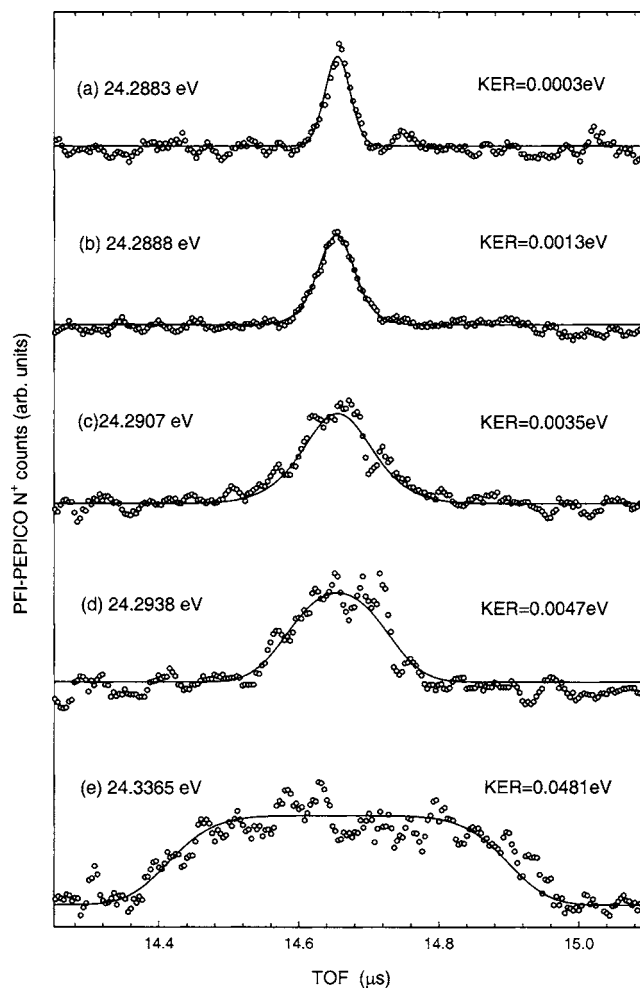


FIG. 5. Selected PFI-PEPICO TOF spectra for N^+ at the VUV photon energies of (a) 24.2883, (b) 24.2888, (c) 24.2907, (d) 24.2938, and (e) 24.3365 eV. The simulated spectra are shown as solid lines. The N^+ peaks are centered at 14.65 μ s.

TOF measurements, the 0-K AE(N^+) from N_2 is found to be 24.2888 ± 0.0010 eV. By taking the narrowest width of the PFI-PEPICO TOF peak for N^+ to mark the threshold for process (1), we obtain the 0-K AE(N^+) = 24.2883 ± 0.0010 eV. The KER analysis for process (1) as summarized in Table I gives the AE(N^+) = 24.2880 ± 0.0009 eV. From these, we recommended the final value of 24.2884 ± 0.0010 eV for the 0-K AE(N^+) of process (1).

TABLE I. Total kinetic-energy releases (KER) and 0-K AE values for reaction (1) measured at selected VUV photoionization energies ($h\nu$).

$h\nu$ (eV)	KER (eV)	0-K AE ^a (eV)
24.2883	0.0003	24.2880
24.2888	0.0013	24.2875
24.2907	0.0035	24.2872
24.2938	0.0047	24.2891
24.3365	0.0481	24.2884
		24.2880 ± 0.0009^b

^aCalculated using Eq. (6).

^bAverage value for the 0-K AE; the quoted uncertainty is the corresponding 95% confidence interval.

Using the latter 0-K AE(N⁺) and the known IE(N₂) = 125 668.00 ± 0.25 cm⁻¹ or 15.580 85 ± 0.000 03 eV (Ref. 17) and IE(N) = 14.534 14 eV (Ref. 15), one straightforwardly obtains by sequential propagation $D_0(\text{N}-\text{N}^+) = 8.7076 \pm 0.0010$ eV and $D_0(\text{N}-\text{N}) = 9.7543 \pm 0.0010$ eV. The latter bond dissociation energy in turn leads to $\Delta H_{f0}^\circ(\text{N}) = 112.469 \pm 0.012$ kcal/mol and, with IE(N), to $\Delta H_{f0}^\circ(\text{N}^+) = 447.634 \pm 0.012$ kcal/mol.

The optical excitation of N₂ in the X¹Σ_g⁺ ground electronic state was found to lead to dissociation with a threshold at 12.139 eV.¹⁵ Thus, the D₀(N–N) can be calculated if the states of the product N atoms are known. Herzberg had narrowed down the possible product states to be N(²D) + N(²D) and N(⁴S) + N(²D),¹⁶ which would yield the corresponding D₀(N–N) values of 9.756 and 7.373 eV. Assuming that the predissociation of the N₂(C³Π_u) state produces N(⁴S_{3/2}) + N(²D_{5/2}) [N(⁴S_{3/2}) + N(²D_{3/2})], a value of 9.759 eV (9.757 eV) can be deduced.¹⁶ The value D₀(N–N) = 9.7543 ± 0.0010 eV obtained in the present study, while in relatively good agreement (i.e., within their uncertainty) with D₀(N–N) = 78 715 ± 50 cm⁻¹ (9.7594 ± 0.0062 eV) reported^{21,22} by Buttenbender and Herzberg, represents an important experimental refinement of this quantity. The currently accepted values for ΔH_f[∘](N) and ΔH_f[∘](N⁺) (e.g., those found in the JANAF Thermochemical Tables²⁰ or in the NIST Web Book¹⁸) are based on the D₀(N–N) value of Buttenbender and Herzberg, as originally suggested by the CODATA Review¹⁹ of Cox *et al.*, which recommends ΔH_{f298.15}[∘](N) = 112.970 ± 0.096 kcal/mol, implying ΔH_{f0}[∘](N) = 112.528 ± 0.096 kcal/mol. Our new value, ΔH_{f0}[∘](N) = 112.469 ± 0.012 kcal/mol, obtained by sequential propagation of the measured appearance energy of N⁺ from N₂, is slightly lower and about eight times more accurate than the currently used value. Inserting the present measurements of the appearance energy of N⁺ from N₂ into the C(A)TN, together with other relevant determinations, and analyzing and solving the full complement of thermochemical interdependencies using Active Thermochemical Tables leads to a very similar value for ΔH_f[∘](N). This fully optimized recommended value obtained through ATcT (and the related discussion) will be the topic of a separate forthcoming report.⁴⁰

IV. SUMMARY

We have conducted a high-resolution PFI-PEPICO TOF study of the dissociative photoionization process of N₂. The 0-K AE(N⁺) values for process (1) deduced based on the breakdown curves of N⁺ and N₂⁺ and the KER analysis of the N⁺ PFI-PEPICO TOF peaks are in agreement. We recommend the average value of 24.2884 ± 0.0010 eV for the 0-K AE(N⁺) from N₂. The latter value has allowed the determination of more precise values for the D₀(N–N), D₀(N⁺–N), ΔH_{f0}[∘](N), and ΔH_{f0}[∘](N⁺).

ACKNOWLEDGMENTS

This work was supported by the U.S. Department of Energy, Office of Basic Energy Sciences, Division of Chemical Sciences, Geosciences, and Biosciences under Contracts No. DE-FG02-02ER15306 (UC Davis) and W-31-109-ENG-38

(Argonne). One of the authors (C.Y.N.) also acknowledges partial supports by the AFOSR Grant No. F49620-03-1-0116 and NSF ATM 0317422. Another author (B.R.) also acknowledges partial support and effort from the numerous team members of the Collaboratory for Multi-Scale Chemical Science (CMCS), which is a project within the National Collaboratories Program sponsored by the U.S. Department of Energy's Division of Mathematical, Information, and Computational Sciences. Portions of this research are related to the effort of a Task Group of the International Union of Pure and Applied Chemistry (2003-024-1-100), which focuses on the thermochemistry of chemical species implicated in combustion and atmospheric chemistry.

¹C. Y. Ng, *Annu. Rev. Phys. Chem.* **53**, 101 (2002).

²G. K. Jarvis, K.-M. Weitzel, M. Malow, T. Baer, Y. Song, and C. Y. Ng, *Rev. Sci. Instrum.* **70**, 3892 (1999).

³K.-M. Weitzel, M. Malow, G. K. Jarvis, T. Baer, Y. Song, and C. Y. Ng, *J. Chem. Phys.* **111**, 8267 (1999).

⁴G. K. Jarvis, K.-M. Weitzel, M. Malow, T. Baer, Y. Song, and C. Y. Ng, *Phys. Chem. Chem. Phys.* **1**, 5259 (1999).

⁵K.-M. Weitzel, G. Jarvis, M. Malow, T. Baer, Y. Song, and C. Y. Ng, *Phys. Rev. Lett.* **86**, 3526 (2001).

⁶Y. Song, X.-M. Qian, K.-C. Lau, C. Y. Ng, J. B. Liu, and W. W. Chen, *J. Chem. Phys.* **115**, 2582 (2001).

⁷Y. Song, X.-M. Qian, K.-C. Lau, C. Y. Ng, J. B. Liu, and W. W. Chen, *J. Chem. Phys.* **115**, 4095 (2001).

⁸Y. Song, X.-M. Qian, K.-C. Lau, and C. Y. Ng, *Chem. Phys. Lett.* **347**, 51 (2001).

⁹X.-M. Qian, Y. Song, K.-C. Lau, C. Y. Ng, J. Liu, and W. Chen, *Chem. Phys. Lett.* **347**, 51 (2001).

¹⁰X.-M. Qian, Y. Song, K.-C. Lau, C. Y. Ng, J. B. Liu, W. W. Chen, and G. Z. He, *Chem. Phys. Lett.* **353**, 19 (2002).

¹¹B. Ruscic *et al.*, *J. Phys. Chem. A* **106**, 2727 (2002).

¹²J. Liu, W. Chen, M. Hochlaf, X. Qian, C. Chang, and C. Y. Ng, *J. Chem. Phys.* **118**, 149 (2003).

¹³X.-M. Qian, K.-C. Lau, G.-Z. He, C. Y. Ng, and M. Hochlaf, *J. Chem. Phys.* **120**, 8476 (2004).

¹⁴X. M. Qian, K. C. Lau, and C. Y. Ng, *J. Chem. Phys.* **120**, 11031 (2004).

¹⁵D. R. Lide, in *Handbook of Chemistry and Physics*, edited by D. R. Lide (CRC, Boca Raton, FL, 1992), p. 10.

¹⁶J. W. McConkey and J. A. Kernahan, *Phys. Lett.* **27**, 82 (1968).

¹⁷F. Merkt and T. P. Softley, *Phys. Rev. A* **46**, 302 (1992).

¹⁸The NIST Chemistry WebBook; <http://webbook.nist.gov/chemistry/>.

¹⁹J. D. Cox, D. D. Wagman, and V. A. Medvedev, *CODATA Key Values for Thermodynamics* (Hemisphere, New York, 1984), p. 1.

²⁰NIST-JANAF Thermochemical Tables (J. Phys. Chem. Ref. Data Monogr 9), 4th ed., edited by M. W. Chase, Jr., (1998), p. 1600.

²¹ICSU-CODATA Task Group, *J. Chem. Thermodyn.* **4**, 331 (1972).

²²G. Buttenbender and G. Herzberg, *Ann. Phys.* **21**, 577 (1935).

²³Y. Tanaka, M. Ogawa, and A. S. Jursa, *J. Chem. Phys.* **40**, 3690 (1964).

²⁴A. G. Gaydon, *Dissociation Energies and Spectra of Diatomic Molecules*, 3rd ed. (Chapman and Hall, London, 1968).

²⁵A. Lofthus and P. H. Krupenie, *J. Phys. Chem. Ref. Data Monogr.* **6**, 113 (1977).

²⁶B. Ruscic *et al.*, *J. Phys. Chem. A* **108**, 9979 (2004).

²⁷B. Ruscic, in *2005 Yearbook of Science and Technology* (McGraw-Hill, New York, 2004), pp. 3–7.

²⁸See, for example, L. A. Curtiss, K. Raghavachari, P. C. Redfern, and J. A. Pople, *J. Chem. Phys.* **106**, 1063 (1997).

²⁹See, for example, J. M. L. Martin and G. de Oliveira, *J. Chem. Phys.* **111**, 1843 (1999).

³⁰P. Heimann, M. Koike, C.-W. Hsu, M. Evans, K. T. Lu, C. Y. Ng, A. Suits, and Y. T. Lee, *Rev. Sci. Instrum.* **68**, 1945 (1997).

³¹C.-W. Hsu, M. Evans, C. Y. Ng, and P. Heimann, *Rev. Sci. Instrum.* **68**, 1694 (1997).

- ³²C. Y. Ng, in *Photoionization and Photodetachment*, Advanced Series in Physical Chemistry, edited by C. Y. Ng, Vol. 10A (World Scientific, Singapore, 1999), Chap. 9, p. 394–538.
- ³³S. Stimson, Y.-J. Chen, M. Evans, C.-L. Liao, C. Y. Ng, C.-W. Hsu, and P. Heimann, *Chem. Phys. Lett.* **289**, 507 (1998).
- ³⁴T. Baer, Y. Song, J. B. Liu, W. W. Chen, and C. Y. Ng, *Faraday Discuss.* **115**, 137 (2000).
- ³⁵J. Liu, M. Hochlaf, and C. Y. Ng, *J. Chem. Phys.* **118**, 4487 (2003).
- ³⁶G. Jarvis and C. Y. Ng (unpublished).
- ³⁷M. Evans, C. Y. Ng, C.-W. Hsu, and P. Heimann, *J. Chem. Phys.* **106**, 978 (1997).
- ³⁸D. A. Dahl, in *Proceedings of the 43rd ASMS Conference on Mass Spectrometry and Allied Topics*, Atlanta, GA, 21-26 May 1995 (unpublished) p. 717.
- ³⁹X.-M. Qian *et al.*, *Rev. Sci. Instrum.* **74**, 4096 (2003).
- ⁴⁰B. Ruscic, R. E. Pinzon, X. Tang, Y. Hou, and C. Y. Ng (unpublished).